DOWNWELLING DIFFUSE ATTENUATION COEFFICIENTS FROM *IN SITU* MEASUREMENTS OF DIFFERENT WATER TYPES

Bisman Nababan[1*], Veronica S.A. Louhenapessy[1], and Risti E. Arhatin[1]
[1]Department of Marine Science and Technology, Faculty of Fisheries and Marine Science, Bogor Agricultural University, Bogor
[*]e-mail: bisman@ipb.ac.id; simson_naban@yahoo.com

Abstract. Process of light reduction or loss (attenuation) by scattering and absorption is affected by solar zenith, time, depth, and seawater constituents. Downwelling diffuse attenuation coefficient (K_d) is important to understand for light penetration and biological processes in ocean ecosystem. It is, therefore, important to know the K_d value and its variability in ocean ecosystem. The objective of this study was to determine downwelling diffuse attenuation coefficients and its variability form in situ measurements of different water types. *In situ* downwelling irradiances (E_d) were measured using a submersible marine environmental radiometer instrument (MER) during a clear sky, calm water condition, and at the time range of 10:30 a.m. up to 14:00 p.m. local time in the northeastern Gulf of Mexico in April 2000. In general, E_d values decreases exponentially with depth. E_d at 380 nm exhibited the lowest attenuation (the most penetrative light), while E_d at 683 nm exhibited the highest attenuation (the most light loss at the top of water column). Overall, the K_d patterns tended to decrease from 380 nm to 490 nm (blue-green wavelength), and increase from 490 nm to 683 nm (green-red wavelength). K_d values in offshore region were relatively lower than in coastal region. K_d can be used to determine the depth of euphotic zone in offshore or teh case-1 water type and the depth of one optical depth (the water column depth where the ocean color satellite can possibly sense).

Keywords: *E_d, K_d, euphotic zone, one optical depth, NEGOM.*

1 INTRODUCTION

The downwelling diffuse attenuation coefficient (K_d) is an important element of seawater optical properties related to light penetration and availability in aquatic ecosystems. The determination of K_d is critical to understand not only physical processes such as the heat transfer in the upper layer of the water column (Nechad and Ruddick, 2010; Wu *et al*., 2007; Lee *et a*l., 2007, 2005; Kirk, 1994; Mobley, 1994; Morel and Antoine, 1994; Sathyendranath *et al*., 1991; Lewis *et al*., 1990), but also biological processes such as phytoplankton photosynthesis and primary production in the ocean euphotic zone (Nechad and Ruddick, 2010; Kirk, 1994; Mobley, 1994; Platt *et al*., 1988; Sathyendranath *et al*., 1989).

K_d is generally defined as the diffrentiation of downwelling irradiances between two layers (depths) as formulated as follows:

$$K_d(z, \lambda) = - \frac{1}{Ed(\lambda)} \frac{dEd}{dz} \quad (1)$$

where K_d (z,λ) is downwelling diffuse attenuation coefficient (m^{-1}), E_d (λ) is downwelling irradiance (W m^{-2}); and *z* is water column depth (m).

As a penetrative component of solar radiation, K_d is affected by depth, solar zenith, time, and seawater constituents (Lee *et al*., 2002, 2005, Mobley, 1994, Kirk, 1994). The effect of solar zenith (elevation) on K_d is relatively small in the lower (blue-green or <500 nm) wavelengths and relatively larger in the higher (yellow-green-red or >500 nm) wavelength (Lee *et al*., 2002; Stramska and Frye, 1997; Kirk, 1991; Gordon, 1989). K_d can also be used to derive water clarity by determining the ability of light transmission (penetration) in the water column using Secchi disc equipment with the following equation:

$$K_d = k/SD \quad (2)$$

where SD is *Secchi Depth* (m) and k is assumed ot be constant (Jamu *et al.* 1999).

From the above equation, it can be concluded that the deeper the secchi disc oberved from the surface water, the clearer the seawater or the smaller the value of K_d.

Approximately 90% of the diffuse reflected light from a water body comes from a surface layer of water within a depth of $1/K_d$ (Lee *et al*., 2002). This condition can also be interpreted that the ocean color satellite can only sense the seawater column at the most within the depth of $1/K_d$. Therefore, K_d is an important parameter for remote sensing reflectance (R_{rs}) of ocean color satellite.

Liu *et al*. (2005) correlated the diffuse attenuation coefficient with seawater quality parameters such as total suspended solid (TSS), Secchi Depth (SD), and salinity. They found that SD measurements had a negative linear relationship with K_d, salinity with positive linear relationship, and no good relationship with TSS. Jacobson (2005) found that variability of K_d was more significantly affected by chlorophyll-a concentration than TSS concentration variabilities. K_d had the highest correlation with chlorophyll-a concentration at 443 nm wavelength (r^2=0.65), while the highest correlation of Kd with TSS found at 710 nm wavelength (r^2=0.4).

Mishra *et al*. (2005) reported that from *in situ* measurments in Roatan island waters the diffuse attenuation coefficient values were relatively low in the blue and green wavelength, and increase above 750 nm.

Informations related K_d values and its variabilites are considered very little, while the use of K_d informations are increasingly important specifically for the use and development of bio-optical model algorithms in ocean color satellites. Therefore, the information of K_d values and its variability is very important. The objective of this study was to determine downwelling diffuse attenuation coefficients and its variability form in situ measurements of different water types.

2 MATERIALS AND METHOD

2.1 Study area

The study was conducted in the region of Northeastern Gulf of Mexico (NEGOM) extending from the Mississippi River Delta to the West Florida Shelf off Tampa Bay within coordinate of 27°18’ - 30°42’ N and 82°36’ - 89°36’ W (Figure 1). In situ downwelling irradiance measurements were conducted in April 2000 and concentrated in four designated region i.e., coastal region or case-2 water (A; stations 3, 4, 12, and 13), continental shelf region or transition from case-2 to case-1 water (B; stations 7 and 15 and C; stations 8, 10, and 11) , and offshore region or case-1 water (D; stations 1, 2, 5, 6, 9, 14, and 16). The study regions limited within 10 m isobath in coastal region up to 1000 m isobath in offshore (Figure 1).

2.2 *In situ* data collection

The data used in this study were the *in situ* measurements of downwelling irradiance (E_d) at various depths in April 2000. The data were used to calculate the value of the downwelling diffuse attenuation coefficients (K_d). Downwelling irradiances (E_d) were collected using a submersible marine environmental radiometer instrument (MER). Before measurements in the field, the MER euipment was calibrated in the laboratory. Dark measurments were also conducted during the night time for dark current calibration. The measurements were casted from the ship deck during a relatively calm water condition (wave height < 0.5 m), relatively clear sky (cloud covered < 30%), and from about 10:30 a.m. to 14:00 p.m. local time.

Data measured by the equipments were upwelling radiance (L_u), downwelling radiance (L_d), upwelling irradiance (E_u), and downelling irradiance (E_d) for wavelength of 380 nm, 412 nm, 443 nm, 455 nm, 475 nm, 490 nm, 510 nm, 532 nnm, 555 nm, 589 nm, 665 nm, 683 nm, and Photosynthetically Active Radiation (PAR).

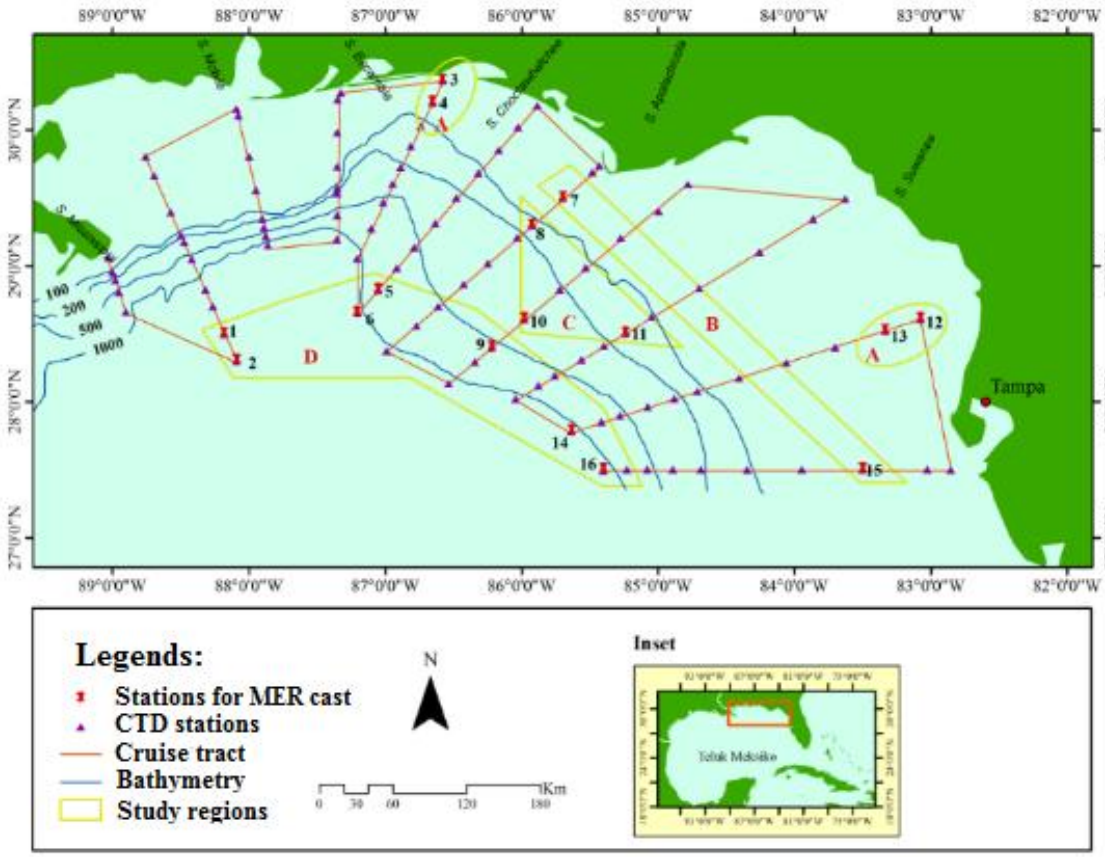

Figure 1. Study area map exhibited the four groups of in situ measurement of coastal region or case-2 water (A), continental region or mixture/transition of case-1 and case-2 waters (B and C), offshore region or case-1 water (D).

Data were recorded for both upcast and downcast. In this study, we used downcast data of downwelling irradiances measurements. The downcast could be extended up to the maximum of 250 m deep with 0.5 m integration depth.

Locations of data collection were divided into four locations i.e., region A (stations 3, 4, 12, and 13), region B (stations 7 and 15), region C (stations 8, 10, and 11), and region D (stations 1, 2, 5, 6, 9, 14, and 16). Region A represented the coastal water typeor case-2 water type, region B and C represented the misture/transition od coastal water and offshore water or mxture/transition of case-2 and case-1 water type, while region

C represented offshore water or case-1 water type. The division was done based on the location of stations where downwelling irradiance measurements were taken and it was assumed that within one region the water constituents or type were similar. We compared the K_d values at the locations of different water type.

2.3 Data Analyses

Raw MER data were processed through standard processing MER data by coverting binary data to csv format data applying dark current calibration and laboratory standard calibration. Data were also fitted using curve fitting tool to eliminate noise caused by ship movement during casting. Exponential equation of E_d produced by fitting processing was used to ixtrapolate E_d at the surface. The compensation depth (the depth where downwelling irradiances remain 1% of downwelling irradiance received at the surface) and depth of one optical depth were also determined using the following equations:

$$Z_\lambda\,(1\%) = \frac{4.6}{Kd(z,\lambda)} \quad \text{..... (3)}$$

$$1\zeta\,(\text{m}) = \frac{1}{Kd(z,\lambda)} \quad \text{..... (4)}$$

where Z_λ (1%) is the compensation depth, 1ζ (m) is the depth of one optical depth, and K_d is the downwelling diffuse attenuation coefficient.

Kruskal-Wallis test was used to determine the significant different of K_d mean values among different region or different water types.

3 RESULTS AND DISCUSSION

3.1 Downwelling irradiance (E_d)

In general, E_d values were exponentially decrease with depth and significantly decrease at the top layer of the water column (Figure 2). E_d graphs at the four represented stations (region) exhibited similar pattern that decreases exponentially with depth. However, the results showed that the gradient of E_d at the red wavelength (> 600 nm) declined sharper than in the blue-green wave length (<600 nm). This occurrred because the water body absorbed more in red wavelength than in the blue-green wavelength range (Kirk, 1994, Moblye, 1994).

The sharp decrease of E_d at the top layer of water column occurred as a result of quick absorption of water body and scattering of light due to present of suspended materials and dissolved organic matter in this layer (Figure 2). In station 3 and 8 (Figure 2), the E_d plots were sharply decrease at the top layer of the water column as a result of the relatively high concentartion of suspended materials and dissolved organic matter originated from riverine input near to the stations such as Choctawhatchee and Escambia River located near to station 3 and Apalachicola river located near to the station 8 (Nababan *et al*., 2011; Nababan, 2005). Phytoplankton biomass that in general higher in the coastal region than in the offshore also helped light attenuation due to its scattering and absorption specifically in blue-green wavelength in the top layer of the water column (Zhai *et al*. 2011; Nababan *et al*., 2011, 2009; Mishra *et al*., 2005). The chlorophyll-a concentrations in the region A were generally >1 mg/m^{-3} or high productivity (Nababan *et al*., 2011; Nababan, 2005).

Location D was a region with generally low primary productivity (phytoplankton <1 mg/m-3). The stations in this region were far enough from the coast resulted in low nutrient from riverine inflow. Therefore, relatively low chlorophyll-a concentration and low organic matter in this region produced less absorption and scattering by phytoplankton and organic matter, causing E_d gradient less sharp compared with E_d in station A, B, and C. NEGOM waters are strongly influenced by large rivers that flow into the region. The large flow of waters from rivers brought particles and nutrients from the mainland into the coastal region in the NEGOM and affecting E_d profile (Nababan *et al*., 2011; Nababan, 2005).

In general, E_d of 380 nm of all stations exhibited similar patterns and had the lowest gradient energy changes indicating the strongest light penetration. Meanwhile, Ed of 665 and 668 nm of all stations exhibited similar patterns and had the highest gradient energy changes indicating the weakest light penetration or the strongest light absorbed by water (Figure 2).

The patterns of E_d on each station within the same region were in general similar, while the patterns of E_d on each station within different region exhibited some differences in the values and their slopes indicating different water type and water constituents in different regions (Figure 2).

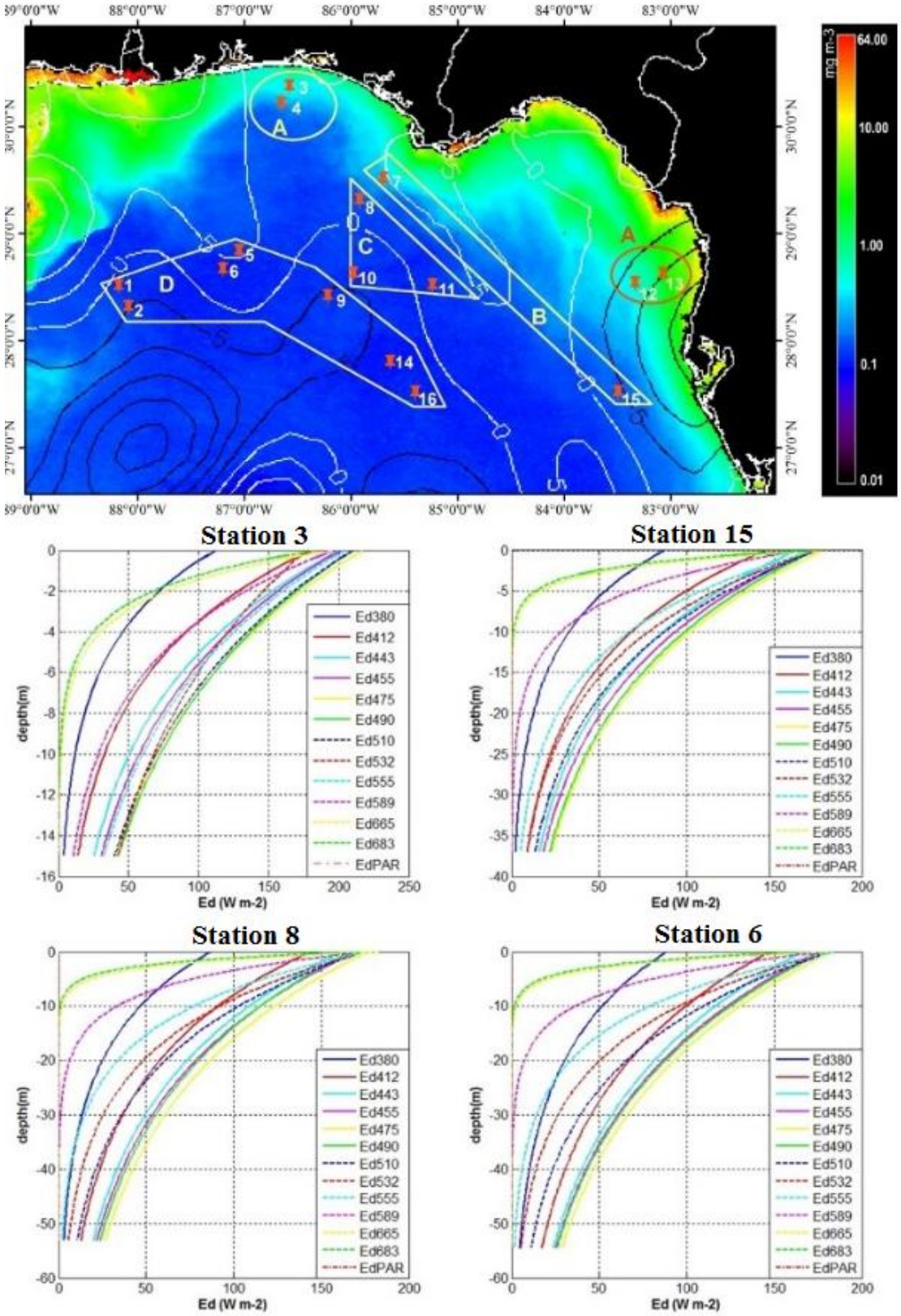

Figure 2. Some examples of downwelling irradiance E_d plots representing the four groups of stations (region). Station 3 represents coastal region or case-2 water type, stations 15 and 8 represent conctinental shelf region or transition between case-1 and case-2 water type, station 6 represents offshore region or case-1 water type.

3.2 Attenuation coefficient (K_d)

In general, attenuation coefficient values at each station exhibited a decrease trend in the range of 380-490 nm and followed by an increase trend in the range of 490-683 nm (Figure 3). The highest value of K_d occurred at the red wavelength (665 and 683 nm) as a result of the sharpest gradient values of Ed specifically at the top layer of water column (see Figure 2). Similar K_d patterns were reported by Mishra *et al*. (2005) showing an increase pattern in the red wavelength and and decrease trend in green-blue wavelength.

In each station, the lowest Kd value was generally found at the green wavelength of 490 nm and the highest Kd value was generally found at the red wavelength of 683 nm (Figure 3). The lowest Kd value (0.014 m^{-1}) at 490 of all station was found at station 1 and 5 of region D where the clearest or case-1 water type was found, while the highest K_d value (0.137 m^{-1}) was found at station 12 of region A where the possible highest suspended material and organic matter or case-2 water type was found (Figure 3).

In region A (coastal water), Kd values of station 3 ranged of 0.050 - 0.096 m^{-1}, station 4 with range of 0.039 - 0.101 m^{-1}, station 12 with range of 0.048 - 0.058 m^{-1}, and station 13 with range of 0.069 - 0.137 m^{-1}. Overall, the K_d values of all stations in region A were relatively higher than in all other stations of region B, C, and D. This occurred due to the highest suspended materials and organic matters found in this region. Brito *et al*. (2013) also reported that in general the highest K_d values were found in shallow water near to the estuari and river mouth.

In region B, K_d values of station 7 ranged of 0.031 - 0.037 m^{-1} and station 15 in range of 0.026 - 0.060 m^{-1}. In region C, K_d values of station 8 ranged of 0.016-0.025 m^{-1}, station 10 with range of 0.015-0.036 m^{-1}, and station 11 with range of 0.017-0.030 m^{-1}. Regions B and C were a transition region from coastal water to offshore water. Therefore, the water properties in this region was a transition between case-1 water and case-2 water.

In region D (offshore water), K_d values at station 1, 2, 5, 6, 9, 14, and 16 ranged of 0.014-0.022 m^{-1}, 0.016-0.039 m^{-1}, 0.014-0.017, 0.016-0.032 m^{-1}, 0.017-0.040, 0.018-0.049 m^{-1}, and 0.016-0.018 m^{-1}, respectively. Overall, Kd values in this region were relatively low compared to other regions (A, B, and C).

K_d values of PAR wavelength in region A ranged of 0053-0096 m^{-1}, while in other regions (B, C, and D), K_d values ranged of 0015-0033 m^{-1} (Figure 3). The average values of K_d of 380-683 nm and Kd PAR in each station of all regions are presented in Table 1. This Table showed that the average values of Kd PAR and K_d 380-683 nm were not significantly different.

Lugo-Fernandez *et al*. (2012) calculated K_d in the northern Gulf of Mexico by dividing the water column into multiple layers, showed that at a depth of <15 meters, K_d ranges from 0.5 - 1.0 m^{-1}, decreased at a depth of 20-100 meters of 0.1 - 0.3 m^{-1}, and above 100 meters obtained K_d range 0.05 - 0.2 m^{-1}. This showed that a lot of the absorption occurredin the surface layer of water. In addition, the results showed that the K_d in coastal waters was greater than the value of K_d in the waters off the coast.

Based on Kruskall-Wallis test and Box & Whisker Plot, K_d values of each wavelength was significantly different within the different regions or different water types i.e., case-1, case-2, and transition water types (significantly different in 95%).

The trend of Kd values decreased from the coastal region toward offshore region, therefore, euphotic zone and the depth of one optical depth increased from from teh coastal region toward offshore region which will be dsiccused in the sub-chapter.

3.3 Euphotic zone and one optical depths

The optical depth is general closely related to water transparency. The cleaer the waters, the deeper the ocean color satellite sensor can sense. Region A was expected to

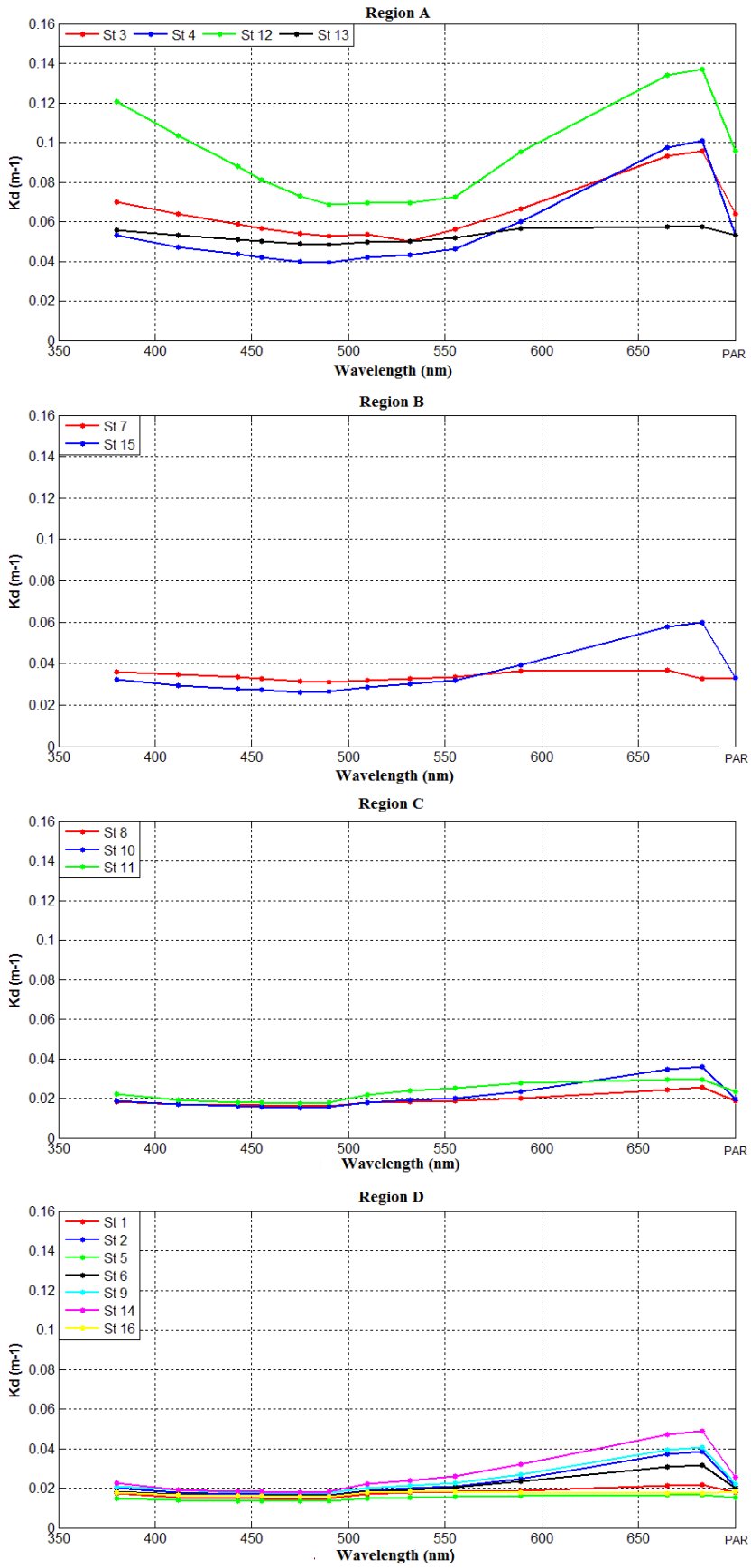

Figure 3. K_d values with respect to wavelength in each station of region A, B, C, and D.

Table 1. Kd PAR and Kd 380-683 average in each station of all regions.

Region	Station	K_d PAR (m^{-1})	Average K_d 380-700 nm (m^{-1})	difference (m^{-1})
A	3	0.0639	0.0643	0.0004
	4	0.0529	0.0546	0.0016
	12	0.0533	0.0526	0.0007
	13	0.0957	0.0927	0.0030
B	7	0.0330	0.0337	0.0007
	15	0.0331	0.0347	0.0016
C	8	0.0187	0.0187	0.0001
	10	0.0197	0.0208	0.0011
	11	0.0234	0.0225	0.0009
D	1	0.0178	0.0171	0.0007
	2	0.0207	0.0221	0.0014
	5	0.0153	0.0149	0.0004
	6	0.0198	0.0203	0.0005
	9	0.0223	0.0234	0.0011
	14	0.0256	0.0262	0.0007
	16	0.0184	0.0171	0.0013

be more turbid than other regions. We derived the euphotic zone based on equation (3) assuming the water depth was limitless. From the calculation, in region A, the depth of euphotic zone depth ranged of 45.5-264.1 m. The results of the euphtoic zone estimation in coastal region were beyond the maximum depth (the maximum depth in region A was about 50 m deep in station 4 and about 30 m in station 12 (Nababan, 2005)). Therefore, the estimation of euphotic zone in coastal region or case-2 water type was not accurate. Meanwhile, the depth of one optical depth in region A (coastal water) ranged of 7.30-25.41 meters. This result indicated the ocean color satellite could sense the water column from surface up to the sea floor in coastal region or case-2 water type. This result also supported theory that ocean color satellite could sense bottom reflectance.

Region B as the transition region had euphtic zone depth in range of 77.1-175.2 m and one optical depth with range of 16.76-38.09 meters (Table 2). The estimation of euphtoic zone in this region was also considered to inaccurate because the maximum depth wtihin region B was less than 100 m (Nababan, 2005). Region C as the transition region had euphotic depth with range of 128.2-298.6 m and one optical depth with range of 27.88 - 64.92 m (Table 2). This zone is closer to the case-1 water type than to the case-2 water type. Therefore, the estimation of euphtoic zone in this region was more reliable. Region D where the highest level of brightness, lowest suspended materials, and lowest organic matter had the depth of euphotic zone in the range of 94.6-340.6 m. This estimation exhibited was more reliable because the maximum depth in thi region was about 500-1000 m deep (Nababan, 2005). Meanwhile, the depth of one optical depth in region D was with the range of 20.57-74.04 m (Table 2). This result indicated that ocean color satellite can sense the water column in this region or the case-1 water type up to 74.04 m. The result also showed that the depth of one optical depth was increase from coastal region toward the offshore region.

Table 2. Range of K_d, the depth of euphotic zone, and the depth of one optical depth.

Regions	Station	K_d (m^{-1})	Depth of euphotic zone (m)	Depth of one optical depth (1ζ) (m)
A	3	0.050 - 0.096	48.0 - 91.5	10.43 - 19.89
	4	0.039 - 0.101	45.5 - 116.9	9.89 - 25.41
	12	0.069 - 0.137	79.9 - 95.4	7.30 - 14.54
	13	0.048 - 0.058	155.8 - 264.1	17.38 - 20.73
B	7	0.031 - 0.037	125.0 - 147.7	27.17 - 32.10
	15	0.026 - 0.060	77.1 - 175.2	16.76 - 38.09
C	8	0.016 - 0.025	180.9 - 288.2	39.34 - 62.66
	10	0.015 - 0.036	128.2 - 298.6	27.88 - 64.92
	11	0.017 - 0.030	155.8 - 264.1	33.87 - 57.41
D	1	0.014 - 0.022	213.7 - 319.6	46.46 - 69.48
	2	0.016 - 0.039	118.9 - 279.2	25.85 - 60.69
	5	0.014 - 0.017	275.2 - 340.6	59.83 - 74.04
	6	0.016 - 0.032	145.9 - 288.8	31.71 - 62.78
	9	0.017 - 0.040	113.6 - 263.4	24.70 - 57.26
	14	0.018 - 0.049	94.6 - 258.2	20.57 - 56.13
	16	0.016 - 0.018	249.1 - 294.3	54.15 - 63.98

4 CONCLUSION

In general, E_d values decreased exponentially with depth. E_d at 380 nm exhibited the lowest attenuation (the most penetrative light), while E_d at 683 nm exhibited the highest attenuation (the most light loss at the top of water column).

Overall, the K_d patterns tended to decrease from 380 nm to 490 nm (blue-green wavelength), and the K_d patterns tend to increase from 490 nm to 683 nm (green-red wavelength). K_d values in offshore region were relatively lower than in coastal region.

Kd can be used to determine the depth of euphotic zone in teh case-1 water type and the depth of one optical depth (the depth where the satellite can possibly sense).

REFERENCES

Brito, A.C., A. Newton, T.F. Fernandes, and P. Tett, 2013, Measuring Light Attenuation in Shallow Coastal Systems, *Journal of Ecosystem and Ecography*, 3:122. doi:10.4172/2157-7625.1000122.

Gilabert, J., A. Perez-Ruzafa, J.M. Gutierrez, A. Bel-Ian, and V. Moreno, 1995, Light attenuation coefficient in shallow coastal waters from airborne multispectral data, *EARSel Advantages in Remote Sensing*, 4(1):76-86.

Gordon, H.R., 1989, Can the Lambert–Beer law be applied to the diffuse attenuation coefficient of ocean water?, *Limnology Oceanography*, 34(8)**:**1,389–1,409 .

Jacobson, E.C., 2005, Light Attenuation in A Nearshore Coral Reef Ecosystems. [thesis]. Hawaii: University of Hawaii, 50p.

Jamu, D.M., Z. Lu, and R.H. Piedrahita, 1999, Relationship between Secchi disk visibility and chlorophyll a in aquaculture ponds, *Aquaculture*, 170:205-214.

Jerlov, N.G., 1976, Marine optics, Amsterdam (NED), Elsevier Scientific Publishing Company. 231p.

Kirk, J.T.O., 1991, Volume scattering function, average cosine, and the underwater light field, *Limnology Oceangraphy*, 36(3):455–467.

Kirk, J.T.O., 1994, Light and photosynthesis in aquatic ecosystem, Second edition, New York: University of Cambridge, 500p.

Lee, Z. P., K. L. Carder, and R. A. Arnone, 2002, Deriving inherent optical properties from water color: A multiple quasi-analytical algorithm for optically deep waters, *Applied Optics*, 41(27):5,755–5,772, doi:10. 1364/AO.41.005755.

Lee, Z. P., M. Darecki, K. Carder, C. Davis, D. Stramski, and W. Rhea, 2005, Diffuse attenuation coefficient of downwelling irradiance: an evaluation of remote sensing methods, *Journal of Geophysical Research: Oceans*, 110, C02017, doi:10.1029/2004JC002573.

Lee, Z. P., K. Du, and R. Arnone, 2005, A model for the diffuse attenuation coefficient of downwelling irradiance, *Journal of Geophyical Research: Oceans*, 110, C02016, doi:10.1029/ 2004JC002275.

Lee, Z. P., A.Weideman, J. Kindle, R. Arnone, K. Carder, and C. Davis, 2007, Euphotic zone depth: Its derivation and implication to ocean-color remote sensing, *Jounal of Geophysical Research: Oceans*, 112, C03009, doi:10.1029/2006JC003802.

Lewis, M., M. Carr, G. Feldman, W.E. Esaias, and C.R. McClain, 1990, Influence of penetrating solar radiation on the heat budget of the equatorial Pacific ocean, *Nature*, 347:543–545, doi:10.1038/347543a0.

Liu, W.C., M.H. Hsu, S.Y. Chen, C.R. Wu, and A.Y. Kuo, 2005, Water column light attenuation in Danshuei river estuary, Taiwan. *Journal of The American Water Resources Association* (JAWRA), 41(2):425-436.

Lugo-Fernandez, A., M. Gravois, R.E. Green, and T. Montgomery, 2012, Examining the mean vertical attenuation scalar quantum irradiance (PAR) over the Lousiana-Texas shelf (northern Gulf of Mexico), *Continental Shelf Research*, 38:24-34.

Mishra, D.R., S. Narumalani, D. Rundquist, and M. Lawson, 2005, Characterizing the vertical diffuse attenuation coefficient for downwelling irradiance in coastal waters: Implications for water penetration by high resolution satellite data, *Journal of Photogrammetry and Remote Sensing*, 60:48-64.

Mobley, C.D., 1994, Light and Water: Radiative Transfer in Natura Waters. San Diego: Academic Press, Inc. 579p.

Morel, A., and D. Antoine, 1994, Heating rate within the upper ocean in relation to its bio-optical state, *Journal of Phyical Oceanography*, 24:1,652–1,665, doi:10.1175/1520-0485(1994) 024.

Nababan, B., 2005, Bio-optical Variability of Surface Water in the Northeastern Gulf of Mexico. [Dissertation]. Florida: University of South Florida. 159p.

Nababan, B., F. E. Muller-Karger, C. Hu, and D. Biggs, 2011, Chlorophyll variability in the Northeastern Gulf of Mexico, *International Journal of Remote Sensing*, 32(23):8,373-8,392.

Nababan, B., 2009, Variability in the light absorption coefficients of phytoplankton, detritus and their relationship with Chlorophyll-a concentration of surface waters, *Journal of National Maritime, 1(Special Edition):41-53*.

Nechad, B., and K. Ruddick, 2010, A model of diffuse attenuation of downwelling irradiance for ecosystem models, *Proceedings of SPIE Vol*. 7858 78580D:1-15.

Platt, T., S. Sathyendranath, C. Caverhill, and M. R. Lewis, 1988, Ocean primary production and available light: further algorithms for remote sensing, *Deep Sea Research Part A. Oceanographic Research Papers*, 35(6):855–879, doi:10.1016/0198-0149(88)90064-7.

Sathyendranath, S., A. D. Gouveia, S. Shetye, P. Ravindran, and T. Platt, 1991, Biological control of surface temperature in the Arabian Sea, *Nature*, 349:54–56, doi:10.1038/ 349054a0.

Sathyendranath, S., T. Platt, C.M. Caverhill, R. Warnock, and M. Lewis, 1989, Remote sensing of oceanic primary production: computations using a spectral model, *Deep Sea Research Part A. Oceanographic Research Papers*, 36(3):431-453, doi:10.1016/ 0198-0149(89)90046-0.

Saulquin, B., A. Hamdi, F. Gohin, J. Populus, A. Mangina, O.F. d'Andona, 2013, Estimation of the diffuse attenuation coefficient K_{dPAR} using MERIS and application to seabed habitat mapping, *Remote Sensing of Environment*, 128:224-223.

Schaeffer, B.A., G.A. Sinclair, Lehrter, M.C. Murrel, J.C. Kurtz, R.W. Gould, and D.F. Yates, 2011, An analysis of diffuse light attenuation in the northern Gulf of Mexico hypoxic zone using the SeaWiFS satellite data record, *Remote Sensing of Environment*, 115(12):3,748-3,757.

Stramska, M., and D. Frye, 1997, Dependence of apparent optical properties on solar altitude: experimental results based on mooring data collected in the Sargasso Sea, *Journal of Geophysical and Reseatch*, 102**:** 15,679–15,691.

Wu, Y., C. Tang, S. Sathyendranath, and T. Platt, 2007, The impact of bio-optical heating on the properties of the upper ocean: A sensitivity study using a 3-D circulation model for the Labrador Sea, *Deep Sea Research Part II*, 54(23):2,630– 2,642, doi:10.1016/j.dsr2. 2007.08.019.

Zhai, L., C. Tang, T. Platt, S. Sathyendranath, 2011, Ocean response to attenuation of visible light in the Gulf of St. Lawrence, *Journal of Marine System*, 88(2):285-297.